Elastic, dielectric, and piezoelectric constants of $Pb(In_{1/2}Nb_{1/2})O_3-Pb(Mg_{1/3}Nb_{2/3})O_3-PbTiO_3$ single crystal poled along $[011]_c$

Enwei Sun,[1,2] Shujun Zhang,[2] Jun Luo,[3] Thomas R. Shrout,[2] and Wenwu Cao[1,2,a)]
[1]*Department of Physics, Harbin Institute of Technology, Harbin 150080, People's Republic of China*
[2]*Materials Research Institute, The Pennsylvania State University, University Park, Pennsylvania 16802, USA*
[3]*TRS Technologies Inc., 2820 East College Avenue, State College, Pennsylvania 16801, USA*

(Received 30 May 2010; accepted 29 June 2010; published online 20 July 2010)

Ternary single crystals $xPb(In_{1/2}Nb_{1/2})O_3-(1-x-y)Pb(Mg_{1/3}Nb_{2/3})O_3-yPbTiO_3$ (PIN-PMN-PT) poled along $[011]_c$ showed remarkable electromechanical properties. We report complete sets of elastic, dielectric, and piezoelectric constants of PIN-PMN-28%PT and PIN-PMN-32%PT, measured by using combined resonance and ultrasonic methods. The electromechanical coupling coefficients k_{15}, k_{32}, and k_{33} can reach 0.95, 0.90, and 0.92, and the piezoelectric strain coefficients d_{15}, d_{32}, and d_{33} are as high as 3354 pC/N, −1781 pC/N, and 1363 pC/N, respectively. These full matrix data sets provide the base for fundamental studies on domain engineering phenomena as well as urgently needed input data for the design of electromechanical devices using $[011]_c$ poled PIN-PMN-PT single crystals. © *2010 American Institute of Physics*. [doi:10.1063/1.3466906]

$[011]_c$-poled relaxor-based ferroelectric single crystals $(1-x)Pb(Zn_{1/3}Nb_{2/3})O_3-xPbTiO_3$ (PZN–xPT) and $(1-x)Pb(Mg_{1/3}Nb_{2/3})O_3-xPbTiO_3$ (PMN–xPT) with compositions near the morphotropic phase boundary (MPB) exhibit ultrahigh transverse piezoelectric properties, which provides the base for much better transverse mode piezoelectric devices.[1–7] However, the coercive field E_C (~2.5 kV/cm) of these binary crystals is too low for high-field driven devices. In addition, their relatively low Curie point T_c (~130–170 °C) and low rhombohedral–tetragonal phase transition temperature T_{R-T} (~75–95 °C) cause poor temperature stability and restrict device operating temperatures.

It was demonstrated that the ternary $xPb(In_{1/2}Nb_{1/2})O_3-(1-x-y)Pb(Mg_{1/3}Nb_{2/3})O_3-yPbTiO_3$ (PIN-PMN-PT) single crystal system has about 30 °C higher rhombohedral–tetragonal phase transition temperature than that of PMN-PT single crystals.[8–10] The coercive field of this ternary single crystal has increased more than twice.[11,12] More importantly, this PIN-PMN-PT single crystal system has just as excellent piezoelectric properties as PMN-PT and PZN-PT single crystals. Recently, Liu *et al.*[13,14] have measured the complete sets of material constants for $[001]_c$- and $[111]_c$-poled rhombohedral PIN-PMN-PT single crystals with MPB composition using combined resonance and ultrasonic methods.

The PIN-PMN-PT ternary relaxor based ferroelectric single crystal has perovskite cubic structure above T_c, becomes tetragonal below T_c and transforms to rhombohedral below T_{R-T} with $3m$ point group symmetry. When the crystal is being poled along $[011]_c$ direction, the domain pattern forms orthorhombic $mm2$ symmetry.[15,16] Following the convention, we take the $[011]_c$ pseudocubic direction as the Z axis, the $[0\bar{1}1]_c$ and $[100]_c$ as the X and Y axes, respectively. Based on such a coordinate choice, we report here two complete sets of material constants for PIN-PMN-28%PT and PIN-PMN-32%PT single crystals poled along $[011]_c$.

The PIN-PMN-PT single crystals used in our work were grown by the modified Bridgman method. The nominal composition of xPIN–$(1-x-y)$PMN–yPT crystals obtained are $x \sim 0.25-0.35$ and $y \sim 0.30-0.32$ but the composition along the growth direction varies due to the segregation of titanium in the crystal. Our crystal samples were cut from the bottom and middle part of the as-grown crystal boule, and the corresponding PT contents are 0.28 and 0.32, respectively.

All samples were oriented using the Laue x-ray machine with an accuracy of ±0.5°. Each sample was cut and polished into a parallelepiped with three pairs of parallel surfaces along $[0\bar{1}1]_c$, $[100]_c$, and $[011]_c$, respectively. Then, the samples were sputtered with gold electrodes on the pair of $[011]_c$ surfaces, and poled with a field of 10–15 kV/cm at room temperature. Because the $[011]_c$ poled multidomain PIN-PMN-PT single crystals have macroscopic orthorhombic $mm2$ symmetry, there are total 17 independent material constants to be determined for each composition; nine elastic, five piezoelectric, and three dielectric constants.

It is nearly impossible to pole samples of different geometries to the same degree because the domain pattern formed depends on the geometry. Therefore, it is often very difficult to get self-consistency full matrix data by using the resonance method described in related textbooks. This is the main reason why some published data on $[011]_c$ poled PMN-PT single crystals measured by using the resonance technique are lack of self-consistency.[17] Therefore, we used combined resonance and ultrasonic methods together with capacitance and d_{33} meter to obtain the maximum number of combinations from the least number of samples.[18]

For resonance measurements, the dimensions and geometries of samples used were specified by the IEEE standards on piezoelectricity.[19] The resonance and antiresonance frequencies were obtained by an HP 4194 A impedance-phase gain analyzer. In ultrasonic measurements, a $5.0 \times 5.0 \times 5.0$ mm^3 cube was used and the orientations are $[0\bar{1}1]_c$,

a)Electronic mail: dzk@psu.edu.

TABLE I. Measured and derived material constants of PIN-PMN-28%PT and PIN-PMN-32%PT multidomain single crystals poled along $[011]_c$. [Directly measured constants are denoted by star (*).]

	Elastic stiffness constants: c_{ij}^E and c_{ij}^D (10^{10} N/m^2)								
	c_{11}^{E*}	c_{12}^E	c_{13}^E	c_{22}^{E*}	c_{23}^E	c_{33}^E	c_{44}^{E*}	c_{55}^{E*}	c_{66}^{E*}
28%PT	19.96	12.51	7.19	13.54	11.89	15.36	6.49	0.76	5.33
32%PT	21.45	15.01	8.01	17.37	14.10	15.26	6.37	0.48	4.56
	c_{11}^D	c_{12}^D	c_{13}^D	c_{22}^D	c_{23}^D	c_{33}^{D*}	c_{44}^{D*}	c_{55}^{D*}	c_{66}^D
28%PT	20.19	12.10	8.26	14.25	10.02	20.21	7.15	4.56	5.33
32%PT	21.50	14.86	8.46	17.94	12.39	20.35	7.30	4.59	4.56
	Elastic compliance constants: s_{ij}^E and s_{ij}^D (10^{-12} m^2/N)								
	s_{11}^{E*}	s_{12}^E	s_{13}^E	s_{22}^{E*}	s_{23}^E	s_{33}^E	s_{44}^E	s_{55}^E	s_{66}^E
28%PT	18.27	−29.36	14.05	69.97	−40.37	31.23	15.41	131.58	18.76
32%PT	25.53	−45.13	27.87	101.45	−70.31	56.84	15.70	208.33	21.93
	s_{11}^D	s_{12}^D	s_{13}^D	s_{22}^D	s_{23}^D	s_{33}^{D*}	s_{44}^D	s_{55}^D	s_{66}^D
28%PT	10.07	−8.75	0.11	18.18	−5.33	7.59	13.99	21.93	18.76
32%PT	11.21	−10.84	1.63	19.37	−7.50	8.79	13.70	21.79	21.93
	Piezoelectric coefficients: $e_{i\lambda}$(C/m^2), $d_{i\lambda}$(10^{-12} C/N), $g_{i\lambda}$(10^{-3} Vm/N), and $h_{i\lambda}$(10^8 V/m)									
	e_{15}	e_{24}	e_{31}	e_{32}	e_{33}	d_{15}	d_{24}	d_{31}^*	d_{32}^*	d_{33}^*
28%PT	16.74	7.39	3.43	−6.00	15.74	2203	114	460	−1156	782
32%PT	16.10	10.32	1.44	−5.50	16.47	3354	162	744	−1781	1363
	g_{15}	g_{24}	g_{31}	g_{32}	g_{33}	h_{15}	h_{24}	h_{31}	h_{32}	h_{33}
28%PT	49.79	12.51	17.80	−44.73	30.26	22.71	8.94	6.79	−11.89	31.20
32%PT	55.63	12.34	19.28	−46.15	35.32	25.51	9.01	2.72	−10.41	31.17
	Dielectric constants: $\varepsilon_{ij}(\varepsilon_0)$ and $\beta(10^{-4}/\varepsilon_0)$											
	ε_{11}^{S*}	ε_{22}^{S*}	ε_{33}^{S*}	ε_{11}^{T*}	ε_{22}^{T*}	ε_{33}^{T*}	β_{11}^S	β_{22}^S	β_{33}^S	β_{11}^T	β_{22}^T	β_{33}^T
28%PT	833	935	570	5000	1030	2920	12.01	10.70	17.54	2.00	9.71	3.43
32%PT	713	1294	597	6814	1483	4361	14.03	7.73	16.75	1.47	6.74	2.29
	Electromechanical coupling factors k_{ij} and density											
	k_{15}	k_{24}	k_{31}^*	k_{32}^*	k_{33}^*	k_t^*	Density (kg/m^3)					
28%PT	0.91	0.30	0.67	0.86	0.87	0.49	8102					
32%PT	0.95	0.36	0.75	0.90	0.92	0.50	8185					

$[100]_c$, and $[011]_c$. A 15 MHz longitudinal wave transducer (Ultran Laboratories, Inc.) and a 20 MHz shear wave transducer (Panametrics Com.) were used for the ultrasonic pulse-echo measurements. The transducers were excited by a 200 MHz pulser/receiver (Panametrics Com.) and the time of flight between echoes was measured using a Tektronix 460 A digital oscilloscope. The phase velocities of the longitudinal and shear waves were measured along the three pure mode directions, i.e., $[0\bar{1}1]_c$, $[100]_c$, and $[011]_c$. We can obtain eight elastic stiffness constants: c_{11}^E, c_{22}^E, c_{33}^D, c_{44}^E, c_{44}^D, c_{55}^E, c_{55}^D, and c_{66}^E based on the Christoffel wave equations from this one sample alone.

From the measured resonance and antiresonance frequencies, we can calculate the corresponding piezoelectric strain coefficients d_{31}, d_{32}, and d_{33}, the elastic compliance constants s_{11}^E, s_{22}^E, s_{33}^E, and s_{33}^D, the elastic stiffness constants c_{33}^D and c_{33}^E, and electromechanical coupling coefficients k_{31}, k_{32}, k_{33}, and k_t. The free and clamped dielectric constants ε_{11}^T, ε_{22}^T, ε_{33}^T, ε_{11}^S, ε_{22}^S, and ε_{33}^S were determined from the low (1 kHz) and high frequency ($2f_a$) capacitance measurements. Overall, we obtained 27 independent measurements for the 17 independent coefficients. A program was developed to extract a reliable self-consistent matrix data set based on error analysis.

The measured and derived elastic, piezoelectric and dielectric constants of the PIN-PMN-28%PT and PIN-PMN-32%PT single crystals poled along $[011]_c$ are given in Table I. Material constants marked with a star (*) were determined directly by the resonance or ultrasonic measurements while others were derived values. Compared with $[001]_c$ poled PIN-PMN-PT single crystal, the main advantage of the $[011]_c$ poled crystal is its super large shear piezoelectric coefficient d_{15} (3354 pC/N for PIN-PMN-32%PT), which is more than an order of magnitude larger than the d_{15} [232

TABLE II. Comparison of some important material constants for different relaxor-based ferroelectric single crystals poled along $[011]_c$.

Single crystals	d_{15} (pC/N)	d_{32} (pC/N)	d_{33} (pC/N)	k_{15}	k_{32}	k_{33}	$\varepsilon_{11}^T/\varepsilon_0$	$\varepsilon_{22}^T/\varepsilon_0$	$\varepsilon_{33}^T/\varepsilon_0$
PMN-28%PT[a]	2816	−1761	1766	0.90	0.89	0.91	7466	4713	6366
PMN-29%PT[b]	1188	−1883	1020	0.83	0.94	0.78	3564	1127	4033
PMN-30%PT[a]	3262	−2116	1916	0.95	0.94	0.92	8783	5233	6966
PIN-PMN-28%PT[c]	2203	−1156	782	0.91	0.86	0.87	5000	1030	2920
PIN-PMN-32%PT[c]	3354	−1781	1363	0.95	0.90	0.92	6814	1483	4361

[a]See Reference 6.
[b]See Reference 7.
[c]This work.

pC/N for PIN-PMN-33%PT (Ref. 13)] of $[001]_c$ poled single crystal.

Some material constants for different relaxor-based ferroelectric single crystals poled along $[011]_c$ are listed in Table II for comparison. We found that the electromechanical coupling coefficients and the piezoelectric strain coefficients of PIN-PMN-32%PT single crystal are comparable to that of PMN-30%PT, much better than PMN-28%PT and PMN-29%PT. The dielectric constants of PIN-PMN-PT system are lower than those of PMN-PT crystal system, making it a better candidate for ultrahigh frequency medical imaging transducers. The coercive field of PIN-PMN-28%PT and PIN-PMN-32%PT is around 5.5 kV/cm, which is more than twice of the value of binary PMN-31%PT (~2.6 kV/cm). Figure 1 shows the temperature dependence of the dielectric constant ε_{33}^T. It can be seen that the Curie temperatures of the PIN-PMN-28%PT and PIN-PMN-32%PT are 165 °C and 192 °C, respectively, which is more than 20 °C higher than that of PMN-31%PT (143 °C). Both the rhombohedral–orthorhombic and orthorhombic–tetragonal phase transition temperatures T_{R-O} and T_{O-T} of PIN-PMN-32%PT (93 °C and 118 °C) are more than 15 °C higher than that of PMN-31%PT (77 °C and 100 °C). For PIN-PMN-28%PT, there is only rhombohedral–tetragonal phase transition, which occurs at T_{R-T}=120 °C.

In summary, by using combined resonance and ultrasonic methods, we have measured the elastic, dielectric, and piezoelectric constants of relaxor-based ferroelectric PIN-PMN-28%PT and PIN-PMN-32%PT ternary multidomain single crystals poled along $[011]_c$. Due to higher phase transition temperature and much larger field endurance, $[011]_c$ poled PIN-PMN-PT single crystals are much better candidates than PMN-PT and PZN-PT single crystals for shear and transverse piezoelectric devices. The two complete sets of material constants for two compositions of $[011]_c$-poled rhombohedral PIN-PMN-PT domain engineered single crystals can be used to perform fundamental theoretical analysis on domain engineering phenomena as well as being the input for finite element packages to design and optimize practical electromechanical device, such as transducers, sensors and actuators.

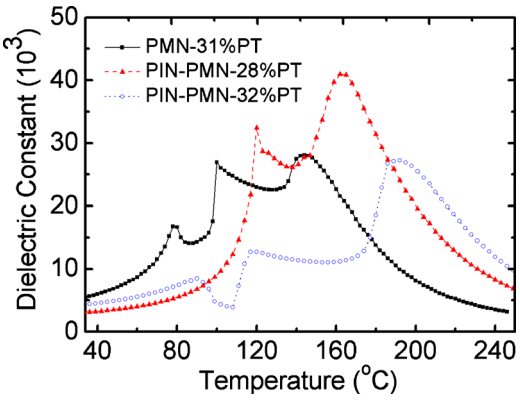

FIG. 1. (Color online) Dielectric constant $\varepsilon_{33}^T/\varepsilon_0$ as a function of temperature for PMN-31%PT, PIN-PMN-28%PT, and PIN-PMN-32%PT single crystals measured in the poling direction $[011]_c$.

This research was supported by the NIH under Grant No. P41-EB21820 and ONR under Grant Nos. N00014-09-01-0456 and N00014-07-C-0858, and the Chinese Ministry of Education for the oversea joint-training Ph.D. student program.

[1]T. Liu and C. S. Lynch, Acta Mater. **51**, 407 (2003).
[2]R. Zhang, B. Jiang, and W. Cao, J. Phys. Chem. Solids **65**, 1083 (2004).
[3]R. Zhang, B. Jiang, W. Jiang, and W. Cao, Appl. Phys. Lett. **89**, 242908 (2006).
[4]K. K. Rajan, M. Shanthi, W. S. Chang, J. Jin, and L. C. Lim, Sens. Actuators, A **133**, 110 (2007).
[5]K. K. Rajan, J. Jin, W. S. Chang, and L. C. Lim, Jpn. J. Appl. Phys., Part 1 **46**, 681 (2007).
[6]M. Shanthi, L. C. Lim, K. K. Rajan, and J. Jin, Appl. Phys. Lett. **92**, 142906 (2008).
[7]F. Wang, L. Luo, D. Zhou, X. Zhao, and H. Luo, Appl. Phys. Lett. **90**, 212903 (2007).
[8]Y. Hosono, Y. Yamashita H, Sakamoto, and N. Ichinose, Jpn. J. Appl. Phys., Part 1 **42**, 5681 (2003).
[9]Y. Hosono, Y. Yamashita, K. Hirayama, and N. Ichinose, Jpn. J. Appl. Phys., Part 1 **44**, 7037 (2005).
[10]S. Zhang, J. Luo, W. Hackenberger, and T. R. Shrout, J. Appl. Phys. **104**, 064106 (2008).
[11]J. Tian, P. Han, X. Huang, H. Pan, J. F. Carroll III, and D. A. Payne, Appl. Phys. Lett. **91**, 222903 (2007).
[12]S. Zhang, J. Luo, W. Hackenberger, N. P. Sherlock, R. J. Meyer, Jr., and T. R. Shrout, J. Appl. Phys. **105**, 104506 (2009).
[13]X. Liu, S. Zhang, J. Luo, T. R. Shrout, and W. Cao, J. Appl. Phys. **106**, 074112 (2009).
[14]X. Liu, S. Zhang, J. Luo, T. R. Shrout, and W. Cao, Appl. Phys. Lett. **96**, 012907 (2010).
[15]D. Viehland, A. Amin, and J. F. Li, Appl. Phys. Lett. **79**, 1006 (2001).
[16]Y. Lu, D.-Y. Jeong, Z.-Y. Cheng, Q. M. Zhang, H. Luo, Z. Yin, and D. Viehland, Appl. Phys. Lett. **78**, 3109 (2001).
[17]V. Yu. Topolov, Appl. Phys. Lett. **96**, 196101 (2010).
[18]R. Zhang, B. Jiang, W. Cao, and A. Amin, J. Mater. Sci. Lett. **21**, 1877 (2002).
[19]ANSI/IEEE Std. 176-1987, *IEEE Standard on Piezoelectricity* (IEEE, New York, 1987), p. 176.